HARQ-Assisted Satellite-Terrestrial Communications Over Generalized-K Fading

Georgios D. Chondrogiannis, *Graduate Student Member, IEEE*, Dimitrios Tyrovolas, *Member, IEEE*, Athanasios P. Chrysologou, *Graduate Student Member, IEEE*, Sotiris A. Tegos, *Senior Member, IEEE*, Antonios Lalas, Konstantinos Votis, Nestor D. Chatzidiamantis, *Member, IEEE*, and George K. Karagiannidis, *Fellow, IEEE*

***Abstract*— Ensuring reliable communication in satellite-terrestrial (S-T) networks, especially under composite fading conditions, is a critical challenge in advancing global connectivity. However, existing literature lacks comprehensive models for such networks, particularly under the Generalized-K (K_G) fading distribution with random ground user deployment. To this end, this work introduces novel closed-form expressions for the outage performance in S-T networks using the Hybrid Automatic Repeat Request with Code Combining (HARQ-CC) protocol. Additionally, the study delves into the network's delay-limited throughput in scenarios of both perfect and imperfect channel feedback. Finally, simulations validate the theoretical findings, demonstrating the HARQ effectiveness in varied fading conditions and feedback reliability.**

***Index Terms*— Satellite communications, hybrid automatic repeat request, imperfect feedback, delay-limited throughput.**

I. Introduction

AS THE development of sixth-generation (6G) networks progresses, the emphasis on achieving widespread coverage is a necessity for supporting advanced applications such as autonomous vehicles, which are integral to broader technological advancements and require reliable and seamless communication [1]. In this direction, non-terrestrial communication nodes like satellites, high-altitude platforms (HAPs), and unmanned aerial vehicles (UAVs) are envisioned as key network components for expanding network coverage [2]. However, global connectivity demands offering mobile services in all locations, including those with harsh propagation conditions characterized by composite fading, where multipath and shadowing effects combine. Therefore, utilizing effective transmission schemes becomes essential, not only for ensuring reliable information transmission and security (e.g. GPS spoofing attack mitigation), but also for establishing a solid foundation for the robust functioning of future vehicle-to-everything (V2X) communication networks.

To achieve global connectivity, especially under composite fading conditions, Hybrid Automatic Repeat Request with Code Combining (HARQ-CC) plays a crucial role in enhancing network reliability through the repeated transmission of encoded messages until acknowledgment (ACK) is received. Recent works [3], [4] underscore the significance of HARQ-CC in these contexts, particularly in enhancing networks' reliability. In this direction, prior research on HARQ-assisted satellite systems has mainly focused on performance analysis using established fading models like the Shadowed-Rician [5] and the Rician distribution [6], with no particular emphasis on the system throughput. In addition, these studies often overlook the practical challenges of imperfect ACK/NACK reception due to the fluctuations of satellite-to-ground channels as well as the potential benefits of exploring other fading models that could offer tractable expressions and insights. Therefore, the unique fading conditions in satellite communications highlight the need for a thorough examination of ductile composite fading models, while also taking into account the impact of imperfect ACK/NACK feedback.

In this work, we delve into the performance of a HARQ-aided satellite-terrestrial (S-T) network under composite fading scenarios. Specifically, for the first time, we derive the statistics of HARQ-CC scheme in closed form, when the channel coefficients are subjected to, the less studied but more versatile, Generalized-K (K_G) distribution model that incorporates a variety of large/small-scale fading scenarios and also aligns with Loo model's precision in depicting S-T channels [7]. Utilizing these results, we analyze the outage performance of a HARQ-assisted S-T network in a K_G composite fading scenario, with randomly distributed users within a coverage area. Additionally, our work investigates the delay-limited throughput (DLT) of the S-T network in the presence of feedback imperfections, which is a key factor in accurately assessing the network's performance under delay constraints. Finally, numerical results verify the accuracy of the provided expressions as well as offer valuable insights that are crucial for improving the design of future HARQ-assisted S-T communication networks.

II. Satellite-Terrestrial Network Overview

A. System and Statistical Models

We consider a downlink S-T network consisting of a Low Earth Orbit (LEO) satellite equipped with a directional antenna

Manuscript received 12 April 2024; revised 28 May 2024; accepted 4 June 2024. Date of publication 12 June 2024; date of current version 14 August 2024. The work in this letter was performed in the frame of the ULTIMO (DOI 10.3030/101077587) project, funded by the European Union under the Horizon Europe research program. The associate editor coordinating the review of this letter and approving it for publication was G. Bacci. *(Corresponding author: Sotiris A. Tegos.)*

Georgios D. Chondrogiannis is with the Department of Electrical and Computer Engineering, Aristotle University of Thessaloniki, 541 24 Thessaloniki, Greece, and also with the Centre for Research and Technology–Hellas (CERTH), Information Technologies Institute, 570 01 Thessaloniki, Greece (e-mail: gchondro@auth.gr).

Dimitrios Tyrovolas, Athanasios P. Chrysologou, Sotiris A. Tegos, and Nestor D. Chatzidiamantis are with the Department of Electrical and Computer Engineering, Aristotle University of Thessaloniki, 541 24 Thessaloniki, Greece (e-mail: tyrovolas@auth.gr; chrysolog@auth.gr; tegosoti@auth.gr; nestoras@auth.gr).

Antonios Lalas and Konstantinos Votis are with the Centre for Research and Technology–Hellas (CERTH), Information Technologies Institute, 570 01 Thessaloniki, Greece (e-mail: lalas@iti.gr; kvotis@iti.gr).

George K. Karagiannidis is with the Department of Electrical and Computer Engineering, Aristotle University of Thessaloniki, 541 24 Thessaloniki, Greece, and also with the Artificial Intelligence and Cyber Systems Research Center, Lebanese American University (LAU), Beirut 03797751, Lebanon (e-mail: geokarag@auth.gr).

Digital Object Identifier 10.1109/LCOMM.2024.3413314

that transmits information packets to ground users (GUs) distributed uniformly within a circular coverage area of radius R. Considering consecutive transmission rounds, as HARQ-CC implies and which will be discussed in the next subsection, the signal received at the j-th transmission round by the i-th GU (GUi) is given by

$$y_{i,j} = \sqrt{l_p P_t G_t G_u} h_j x_t + n_i, \tag{1}$$

where G_t, G_u are the transmitting and receiving antenna gains, respectively, x_t represents the transmitted symbol with $\mathbb{E}\left[|x_t|^2\right] = 1$, and n_i is the complex white Gaussian noise at the GU$_i$ with variance $\sigma^2_{n_i}$, i.e., $n_i \sim \mathcal{CN}(0, \sigma^2_{n_i})$. Moreover, the satellite transmission power is denoted by P_t, and the path loss term $l_p = C_0 d_i^{-a}$ incorporates the distance d_i between the S and GUi, with $C_0 = \left(\frac{\lambda}{4\pi}\right)^2$ refers to the constant term of path loss value at reference distance $d_0 = 1$m, where λ is the wavelength and a represents the path loss exponent. Hence, the instantaneous signal-to-noise ratio (SNR) at GUi is defined as

$$\gamma_{i,j} = \frac{\bar{\gamma}_{\text{tr}} G_u |h_j|^2}{d_i^a}, \tag{2}$$

where $\bar{\gamma}_{\text{tr}} = \frac{C_0 P_t G_t}{\sigma^2_{n_i}}$ represents the average transmit SNR.

Assuming that GUs need to always stay connected with the network, it is of paramount importance to examine the S-T network performance, even in cases where the signal propagation is characterized by severe multipath fading, along with shadowing. Several fading models have been proposed to describe S-T channels [5], [6], [7]. Each model's precision varies with channel conditions and the system's environmental or physical aspects. In this work, the K_G distribution is adopted since it is reported to effectively capture scenarios with significant signal fluctuations caused by atmospheric conditions, varied terrain, and other environmental factors [7]. Thus, assuming that the random variable (RV) $|h_j|$ is K_G distributed, the probability density function (PDF) of the RV $\mu_j = \bar{\mu} |h_j|^2$, where $\bar{\mu} = \bar{\gamma}_{\text{tr}} G_u$ can be expressed as [8].

$$f_{\mu_j}(\mu) = \frac{2\left(\frac{km}{\bar{\mu}}\right)^{\frac{k+m}{2}} \mu^{\frac{k+m}{2}-1}}{\Gamma(k)\Gamma(m)} K_{k-m}\left(2\sqrt{\frac{km}{\bar{\mu}}\mu}\right). \tag{3}$$

where k and m are the distribution's shaping parameters, $\Gamma(\cdot)$ is the gamma function and $K_{k-m}(\cdot)$ is the modified Bessel function of the second kind and order $k-m$.

Furthermore, to accurately evaluate the performance of the studied scenario, the GUs are modeled as a set of independent and uniformly distributed points within a circle of radius R, reflecting the common topology and randomness of user's positions that occurs in an S-T network. To this end, the distance d_i between S at altitude L and the GU$_i$ is assumed to be an RV with PDF given by $f_{d_i}(x) = \frac{2x}{R^2}$, $x \in \left[L, \sqrt{L^2+R^2}\right]$. Finally, after some algebraic manipulations, it follows that the PDF of d_i^a can be expressed as

$$f_{d_i^a}(y) = \frac{2}{aR^2} y^{\frac{2}{a}-1}, \quad y \in \left[L^a, \left(L^2+R^2\right)^{\frac{a}{2}}\right]. \tag{4}$$

B. HARQ-Code Combining (HARQ-CC)

Regarding the need to maintain connectivity with the S-T network, challenges such as atmospheric disturbances, long distances, and physical obstructions can significantly compromise the network's coverage. To address this issue, HARQ-CC with NACK/ACK feedback in each round can be employed as a transmission scheme to enhance the system's robustness. In particular, this scheme involves repeated transmissions of the same encoded message until an ACK is received or the maximum retransmission limit $J_{\max}$ is reached, and at the receiving end, these multiple transmissions are combined using maximal ratio combining (MRC), enhancing the probability of successful decoding. As a result, the accumulated mutual information (MI) [3] after J rounds of HARQ-CC is given by

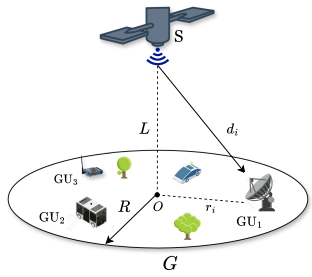

Fig. 1. System's overview.

$$I^{\text{CC}}_{i,J} = \frac{1}{J}\log_2\left(1 + \sum\nolimits_{j=1}^{J} \gamma_{i,j}\right). \tag{5}$$

III. Performance Analysis

In this section, we explore analytical derivations to gain insights into the coverage and throughput of the examined S-T network. Specifically, our focus lies on two key performance metrics: i) the outage probability for a randomly deployed GU using HARQ-CC in K_G fading and ii) the delay-limited throughput, a critical metric in satellite networks due to long link distances, representing the highest transmission rate achievable within finite delay constraints [9]. Additionally, considering the likelihood of imperfect ACK/NACK reception, we provide closed-form expressions for these metrics under the assumption of an imperfect feedback channel.

A. Outage Performance

For the case where a HARQ-assisted system requires J transmission rounds to reach the rate threshold $\mathcal{R}_t$, the achievable rate for this system by the end of these rounds effectively becomes $\mathcal{R}_t/J$. Therefore, the outage probability after J transmission rounds is defined as the probability that $I^{\text{CC}}_{i,J}$ is less than the adjusted rate threshold $\mathcal{R}_t/J$ and can be expressed as

$$\mathcal{P}^{\text{CC}}_{i,J} = \Pr\left(\sum_{j=1}^{J} \gamma_{i,j} < 2^{\mathcal{R}_t} - 1 = \gamma_{\text{th}}\right) = F_{Z_{i,J}}(\gamma_{\text{th}}), \tag{6}$$

where $Z_{i,J} = \sum_{j=1}^{J} \gamma_{i,j}$. From the expression above, it follows that the cumulative density function (CDF) of $Z_{i,J}$ is calculated using the formula for ratio distribution by

$$F_{Z_{i,J}}(z) = \int_{L^a}^{\left(L^2+R^2\right)^{\frac{a}{2}}} F_{\Phi_J}(zy) f_{d_i^a}(y) dy, \tag{7}$$

where Φ_J is defined as the sum of J RVs whose PDF is given in (3). Thus, towards calculating system's outage probability, we firstly determine the CDF of Φ_J, which to the best of our knowledge, has not been addressed in the literature so far.

Proposition 1: Assuming that $|h_j|$ follows the K_G distribution, the overall PDF and CDF of $\Phi_J = \sum_{j=1}^{J} \mu_j$ can be, respectively, expressed as

$$f_{\Phi_J}(\phi) = \sum_{n_1=0}^{\infty} \cdots \sum_{n_J=0}^{\infty} \sum_{u_1=1}^{2} \cdots \sum_{u_J=1}^{2} \Xi_J(\mathbf{n},\mathbf{u})\, \phi^{W_J(\mathbf{n},\mathbf{u})-1}, \quad (8)$$

$$F_{\Phi_J}(\phi) = \sum_{n_1=0}^{\infty} \cdots \sum_{n_J=0}^{\infty} \sum_{u_1=1}^{2} \cdots \sum_{u_J=1}^{2} \frac{\Xi_J(\mathbf{n},\mathbf{u})}{W_J(\mathbf{n},\mathbf{u})}\, \phi^{W_J(\mathbf{n},\mathbf{u})}, \quad (9)$$

where $\Xi_J(\mathbf{n},\mathbf{u})$ is given by (10), as shown at the bottom of the page, with $\mathcal{N}_J = \sum_{l=1}^{J} n_l$ and

$$W_J(\mathbf{n},\mathbf{u}) = \mathcal{N}_J + \sum_{l=1}^{J} \left[\frac{k}{2}\left((-1)^{u_l}+1\right) + m\left((-1)^{u_l-1}+1\right) \right]. \quad (11)$$

Proof: The proof for the derivation of (8) is provided in Appendix. Also, (9) follows straightforwardly from (8). ∎

Proposition 2: The S-T system's outage probability after J HARQ-CC transmission rounds can be expressed as

$$\mathcal{P}_{i,J}^{\mathrm{CC}}(\gamma_{th}) = \sum_{n_1=0}^{\infty} \cdots \sum_{n_J=0}^{\infty} \sum_{u_1=1}^{2} \cdots \sum_{u_J=1}^{2} H_{J,a}(\mathbf{n},\mathbf{u})\, \gamma_{th}^{W_J(\mathbf{n},\mathbf{u})}, \quad (12)$$

with $H_{J,a}$ being equal to

$$H_{J,a}(\mathbf{n},\mathbf{u}) = \frac{2\,\Xi_J(\mathbf{n},\mathbf{u}) \left[\left(L^2+R^2\right)^{\frac{aW_J(\mathbf{n},\mathbf{u})}{2}+1} - L^{aW_J(\mathbf{n},\mathbf{u})+2} \right]}{R^2\left(aW_J^2(\mathbf{n},\mathbf{u}) + 2W_J(\mathbf{n},\mathbf{u})\right)}. \quad (13)$$

Proof: Exploiting (9) and by substituting it into integral (7), after some algebraic manipulations (12) is derived. ∎

Remark 1: In the high-SNR region, the dominant term of the infinite sums is the one with the smallest exponent value, which corresponds to the case of $n_1 = n_2 = \cdots = \mathcal{N}_J = 0$. Therefore, the diversity order of the given outage probability can be easily calculated as $J\min\{k,m\}$.

B. Delay-Limited Throughput

In the context of HARQ-aided communication systems, the long-term average throughput (LTAT) has been derived and studied for both reliable and imperfect feedback conditions in [3]. However, LTAT is incapable of capturing the delay-limited nature of S-T networks. In this direction, we explore the network's DLT, a critical metric defined as the transmission rate achievable under finite delay restrictions across various fading scenarios, without reliance on long-term asymptotic behavior, which is expressed as [9], [10]

$$\mathcal{D}_\eta = \sum_{j=1}^{J_{\max}} \frac{\mathcal{R}_t}{j} P_{s,j}, \quad (14)$$

where $P_{s,J}$ is the probability of successful data reception at the J-th transmission round, and is given as [11]

$$P_{s,J} = \mathcal{P}_{i,J-1} - \mathcal{P}_{i,J}, \quad J = 1,\ldots,J_{\max}. \quad (15)$$

Next, we provide, for the first time, the DLT of the studied network, taking into account the possibility of imperfect ACK/NACK feedback reception, which is crucial for its accurate throughput assessment due to the long distances and physical phenomena encountered in S-T communication.

Proposition 3: The DLT of a system that employs HARQ, under the imperfect feedback assumption, is given as

$$\mathcal{D}_\eta^{if} = \sum_{j=1}^{J_{max}-1} \sum_{q=1}^{j} \frac{(1-\epsilon_f)^q\, \epsilon_f^{j-q} \mathcal{R}_t}{j} P_{s,q} + \sum_{q=1}^{J_{max}} \frac{(1-\epsilon_f)^{q-1}\, \epsilon_f^{J_{max}-q} \mathcal{R}_t}{J_{max}} P_{s,q}, \quad (16)$$

where ϵ_f is the probability of erroneous ACK or NACK reception.

Proof: In scenarios with imperfect feedback from the GU, HARQ process can be considered successful at the j-th round under two distinct circumstances:

a) The packet is successfully received in the j-th round, and the feedback message is also accurately received at the same round. The probability of this occurrence is denoted as $(1-\epsilon_f)^j P_{s,j}$.
b) The packet is successfully received by the receiver at a previous round $q \le j$, and the corresponding ACK/NACK feedback message is accurately received by the transmitter at the j-th round. The probability of this event is given by the term $(1-\epsilon_f)^q \epsilon_f^{j-q} P_{s,q}$.

Consider that if NACK feedback alternates to ACK the HARQ process ends unsuccessfully. Also, it is important to note that if the maximum number of transmissions is reached, the final feedback message does not influence the throughput, as a new packet will be transmitted in the subsequent round. Additionally, the events described above are mutually exclusive, allowing for the summation of their respective probabilities to derive the expression in (16). ∎

Remark 2: By setting $\epsilon_f = 0$ in (16), the DLT reduces to the case of a reliable feedback channel.

IV. Numerical Results

In this section, we analyze the performance of a HARQ-assisted S-T downlink system with randomly-deployed GUs under G_K fading via both analytical (an.) and simulation (sim.) results. Unless otherwise stated, the simulation parameters are set as follows: $J_{\max} = 4$ for the maximum number of retransmissions, path-loss exponent $a = 2$, receiving antenna gain $G_u = 60$ dB, link distance $L = 300$ km, and coverage radius $R = 50$ km. Finally, it is noted that for the calculations

$$\Xi_J(\mathbf{n},\mathbf{u}) = \left(\frac{\pi \left(\frac{km}{\bar{\mu}}\right)^{\frac{k+m}{2}}}{\Gamma(k)\Gamma(m)\sin(\pi(k-m))} \right)^J \frac{1}{\prod_{l=1}^{J}(n_l!)} (-1)^{\sum_{l=1}^{J} \frac{(-1)^{u_l}+1}{2}} \left(\frac{km}{\bar{\mu}}\right)^{\sum_{l=1}^{J}\left(n_l+(-1)^{u_l}\frac{k-m}{2}\right)} \times \frac{1}{\Gamma\left(\sum_{l=1}^{J} \frac{1}{2}\left(((-1)^{u_l}+1)k + ((-1)^{u_l-1}+1)m\right) + \mathcal{N}_J\right)} \prod_{l=1}^{J} \frac{\Gamma\left(\frac{((-1)^{u_l}+1)k + ((-1)^{u_l-1}+1)m}{2} + n_l\right)}{\Gamma\left((-1)^{u_l}k + (-1)^{u_l-1}m + n_l + 1\right)}. \quad (10)$$

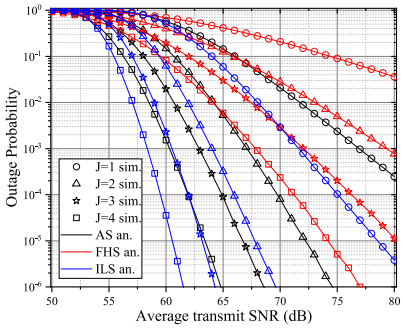

Fig. 2. Outage probability versus Average transmit SNR for different shadowing conditions and values of $J_{\max}$.

TABLE I

CHANNEL PARAMETERS FOR SHADOWING CONDITIONS [7], [12]

Shadowing	k	m
Infrequent light shadowing (ILS)	75.1155	3
Average shadowing (AS)	7.9115	2
Frequent heavy shadowing (FHS)	1.0931	1

of the infinite summations of (12), a number of 30 terms was sufficient. Throughout the provided figures, markers represent sim. and straight lines represent the an. results.

Fig. 2 presents both theoretical and simulation results for the proposed system under various shadowing conditions. These conditions embody a large number of physical phenomena encountered in S-T channels, such as tropospheric scattering and radar clutter [7], which also correspond to various settings already described in 3GPP's technical reports. Specifically, it examines infrequent light shadowing (ILS), average shadowing (AS), and frequent heavy shadowing (FHS), with their parameters detailed in Table I. As it can be observed, HARQ-CC significantly enhances the reliability of the proposed satellite system, even with a low maximum number of retransmissions. Moreover, it can be seen that improved channel conditions correspond to a more pronounced enhancement in outage probability as the limit of maximum retransmission rounds increases. Furthermore, as Remark 1 suggested, it is visible that the curve slopes depend on the parameters J, k and m. Finally, the efficiency of the HARQ protocol often results in a reliability improvement that surpasses the impact of shadow fading conditions, highlighting its ability to maintain performance across different shadowing conditions, and thus, its utility in diverse satellite communication scenarios.

In Fig. 3, the outage performance of the system under study is depicted, focusing on the effects of varying satellite altitude L and coverage radius R. The analytical and simulation results, which coincide, reveal that the size of the coverage area has a minimal impact on the system's outage performance, especially at higher satellite altitudes. This underscores the advantages of using a wider beam for enhanced connectivity, significantly extending the coverage area with minimal impact on system reliability, while in contrast, the satellite's altitude plays a more substantial role in determining outage probability. This highlights a crucial trade-off between altitude and coverage in the design of satellite systems, while indicating that LEO satellites, due to their lower altitudes, potentially provide a more favorable solution for enhanced coverage.

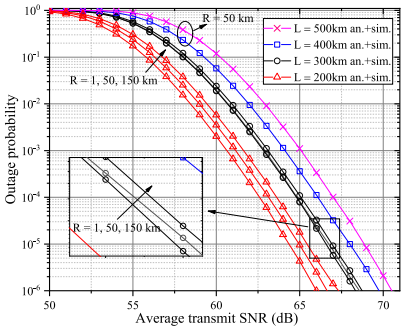

Fig. 3. Outage probability vs Average transmit SNR for different values of altitude L and coverage radius R, with AS conditions.

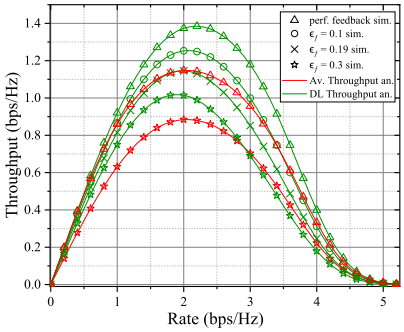

Fig. 4. LTAT and DLT for different values of imperfect feedback versus the transmission rate R_t in AS conditions with $\bar{\gamma}_{\text{tr}} = 60$ dB.

Finally in Fig. 4, DLT and LTAT is presented for the cases of imperfect and reliable $(\epsilon_f = 0)$ feedback at the satellite transmitter, with different values assigned to it. In this scenario, we assume AS condition and a moderate average transmit SNR value, $\bar{\gamma}_{\text{tr}} = 60$ dB. In general, it can be observed that the DLT achieves a higher throughput value than the LTAT under similar conditions. Specifically, in the simulated scenario, the highest value achieved by LTAT can also be achieved by the DLT with imperfect feedback probability equal to $\epsilon_f = 0.19$, at the transmission rate $R_t \simeq 2$ bps/Hz. These particular facts lead us to conclude that the imposition of finite delay constraints in the HARQ-assisted satellite system results in a performance enhancement in terms of guaranteed throughput in all fading states, which comes in handy for several delay-critical applications. A last observation that can be made in Fig. 4 is that the existence of various feedback imperfections (and channel conditions) results in a change of the transmission rate that attains the maximum throughput value, which must be taken into account during the cross-layer design of the proposed system. For instance, as it can be seen for from the figure, the maximum value of DLT without feedback imperfection can be obtained with a transmission rate of $R_t \simeq 2.2$ bps/Hz, while the DLT with $\epsilon_f = 0.3$ is maximized at $R_t \simeq 1.8$ bps/Hz.

APPENDIX
PROOF OF PROPOSITION 1

The proof begins with the calculation of the PDF for the sum of $J = 2$ and subsequently $J = 3$ independent squared K_G RVs and then extends to an arbitrary number J of squared K_G RVs by induction. Specifically, the PDF of the sum of two random variables is calculated by convolution as

$$f_{\Phi_2}(z) = \int_0^z f_{\mu_1}(z-x) f_{\mu_2}(x) dx. \tag{17}$$

$$f_{\Phi_2}(z)=\left(\frac{\pi\left(\frac{km}{\bar{\mu}}\right)^{\frac{k+m}{2}}}{\sin(\pi(k-m))\Gamma(k)\Gamma(m)}\right)^2\sum_{n_1=0}^{\infty}\sum_{n_2=0}^{\infty}\frac{1}{n_1!n_2!}\left(\frac{\left(\frac{km}{\bar{\mu}}\right)^{k+\mathcal{N}_2-m}\Gamma(k+n_1)\Gamma(k+n_2)z^{2k+\mathcal{N}_2-1}}{\Gamma(k+n_1-m+1)\Gamma(2k+\mathcal{N}_2)\Gamma(k+n_2-m+1)}\right.$$
$$-\frac{\left(\frac{km}{\bar{\mu}}\right)^{\mathcal{N}_2}\Gamma(k+n_2)\Gamma(n_1+m)z^{k+\mathcal{N}_2+m-1}}{\Gamma(-k+n_1+m+1)\Gamma(k+n_2-m+1)\Gamma(k+\mathcal{N}_2+m)}-\frac{\left(\frac{km}{\bar{\mu}}\right)^{\mathcal{N}_2}\Gamma(k+n_1)\Gamma(n_2+m)z^{k+\mathcal{N}_2+m-1}}{\Gamma(k+n_1-m+1)\Gamma(-k+n_2+m+1)\Gamma(k+\mathcal{N}_2+m)}$$
$$\left.+\frac{\left(\frac{km}{\bar{\mu}}\right)^{-k+\mathcal{N}_2+m}\Gamma(n_1+m)\Gamma(n_2+m)z^{\mathcal{N}_2+2m-1}}{\Gamma(-k+n_1+m+1)\Gamma(-k+n_2+m+1)\Gamma(\mathcal{N}_2+2m)}\right) \tag{20}$$

$$f_{\Phi_3}(z)=\left(\frac{\pi\left(\frac{km}{\bar{\mu}}\right)^{\frac{k+m}{2}}}{\sin(\pi(k-m))\Gamma(k)\Gamma(m)}\right)^3\sum_{n_1=0}^{\infty}\sum_{n_2=0}^{\infty}\sum_{n_3=0}^{\infty}\frac{1}{n_1!n_2!n_3!}\left(\frac{\left(\frac{km}{\bar{\mu}}\right)^{\mathcal{N}_3-\frac{3(k-m)}{2}}\Gamma(n_1+m)\Gamma(n_2+m)\Gamma(n_3+m)}{\Gamma(n_1-k+m+1)\Gamma(n_2-k+m+1)\Gamma(n_3-k+m+1)}\right.$$
$$\times\frac{z^{\mathcal{N}_3+3m-1}}{\Gamma(\mathcal{N}_3+3m)}+\frac{\left(\frac{km}{\bar{\mu}}\right)^{\mathcal{N}_3+k-m-\frac{k-m}{2}}\Gamma(n_1+k)\Gamma(n_2+k)\Gamma(n_3+m)z^{\mathcal{N}_3+2k+m-1}}{\Gamma(n_1+k-m+1)\Gamma(n_2+k-m+1)\Gamma(n_3-k+m+1)\Gamma(\mathcal{N}_3+2k+m)}-\frac{z^{\mathcal{N}_3+k+2m-1}}{\Gamma(\mathcal{N}_3+k+2m)}$$
$$\times\frac{\left(\frac{km}{\bar{\mu}}\right)^{N_3-\frac{k-m}{2}}\Gamma(n_1+k)\Gamma(n_2+m)\Gamma(n_3+m)}{\Gamma(n_1+k-m+1)\Gamma(n_2-k+m+1)\Gamma(n_3-k+m+1)}-\frac{\left(\frac{km}{\bar{\mu}}\right)^{\mathcal{N}_3-\frac{k-m}{2}}\Gamma(n_1+m)\Gamma(n_2+k)\Gamma(n_3+m)}{\Gamma(n_1-k+m+1)\Gamma(n_2+k-m+1)\Gamma(n_3-k+m+1)}$$
$$\times\frac{z^{\mathcal{N}_3+k+2m-1}}{\Gamma(\mathcal{N}_3+k+2m)}-\frac{\left(\frac{km}{\bar{\mu}}\right)^{\mathcal{N}_3-\frac{k-m}{2}}\Gamma(n_1+m)\Gamma(n_2+m)\Gamma(n_3+k)z^{\mathcal{N}_3+2m+k-1}}{\Gamma(n_1-k+m+1)\Gamma(n_2-k+m+1)\Gamma(n_3+k-m+1)\Gamma(\mathcal{N}_3+2m+k)}-\frac{z^{\mathcal{N}_3+3k-1}}{\Gamma(\mathcal{N}_3+3k)}$$
$$\times\frac{\left(\frac{km}{\bar{\mu}}\right)^{\mathcal{N}_3+\frac{3(k-m)}{2}}\Gamma(n_1+k)\Gamma(n_2+k)\Gamma(n_3+k)}{\Gamma(n_1+k-m+1)\Gamma(n_2+k-m+1)\Gamma(n_3+k-m+1)}+\frac{\left(\frac{km}{\bar{\mu}}\right)^{\mathcal{N}_3+\frac{k-m}{2}}\Gamma(n_1+m)\Gamma(n_2+k)\Gamma(n_3+k)}{\Gamma(n_1-k+m+1)\Gamma(n_2+k-m+1)\Gamma(n_3+k-m+1)}$$
$$\left.\times\frac{z^{\mathcal{N}_3+2k+m-1}}{\Gamma(\mathcal{N}_3+2k+m)}+\frac{\left(\frac{km}{\bar{\mu}}\right)^{\mathcal{N}_3+\frac{k-m}{2}}\Gamma(n_1+k)\Gamma(n_2+m)\Gamma(n_3+k)z^{\mathcal{N}_3+2k+m-1}}{\Gamma(n_1+k-m+1)\Gamma(n_2-k+m+1)\Gamma(n_3+k-m+1)\Gamma(\mathcal{N}_3+2k+m)}\right) \tag{21}$$

Assuming $k-m\notin\mathbb{Z}$ and using [13, (8.485)] with [13, (8.445)], (3) is rewritten as

$$f_{\mu_j}(\mu)=\frac{\pi}{\Gamma(k)\Gamma(m)\sin((k-m)\pi)}$$
$$\times\sum_{l=0}^{\infty}\left(\frac{(km)^{l+m}\left(\frac{\mu}{\bar{\mu}}\right)^{l+m-1}}{l!\,\Gamma(l-k+m+1)}-\frac{(km)^{l+k}\left(\frac{\mu}{\bar{\mu}}\right)^{l+k-1}}{l!\,\Gamma(l+k-m+1)}\right). \tag{18}$$

Thus, by substituting (18) into (17), using [13, (3.191)] and after some manipulations, the PDF of the sum of $J=2$ squared K_G RVs is given by (20), as shown at the top of the page. Similarly, the PDF of the sum of $J=3$ squared K_G RVs can be derived by applying

$$f_{\Phi_3}(z)=\int_0^z f_{\mu_3}(z-x)f_{\Phi_2}(x)dx. \tag{19}$$

To this end, by substituting (20) and (18) into (19), using [13, (3.191)] and after some algebraic manipulations, the PDF of the sum of $J=3$ is given by (21), as shown at the top of the page. Convergence of (20) and (21) is ensured by the convergence of (18) and the fact that summation/integration can be alternated in the definite integrals of (17) and (19). Following the same process for an arbitrary number J of RVs, (8) is derived.

REFERENCES

[1] M. Noor-A-Rahim et al., "6G for vehicle-to-everything (V2X) communications: Enabling technologies, challenges, and opportunities," *Proc. IEEE*, vol. 110, no. 6, pp. 712–734, Jun. 2022.

[2] M. Giordani and M. Zorzi, "Non-terrestrial networks in the 6G era: Challenges and opportunities," *IEEE Netw.*, vol. 35, no. 2, pp. 244–251, Mar. 2021.

[3] A. Chelli et al., "Throughput and delay analysis of HARQ with code combining over double Rayleigh fading channels," *IEEE Trans. Veh. Technol.*, vol. 67, no. 5, pp. 4233–4247, May 2018.

[4] D. Tyrovolas et al., "Slotted ALOHA with code combining for IoT networks," in *Proc. IEEE Int. Mediterr. Conf. Commun. Netw. (MeditCom)*, Sep. 2023, pp. 164–168.

[5] G. Pan et al., "On HARQ schemes in satellite-terrestrial transmissions," *IEEE Trans. Wireless Commun.*, vol. 19, no. 12, pp. 7998–8010, Dec. 2020.

[6] H. Bian and R. Liu, "Reliable and energy-efficient LEO satellite communication with IR-HARQ via power allocation," *Sensors*, vol. 22, no. 8, p. 3035, Apr. 2022.

[7] K. P. Peppas, "Accurate closed-form approximations to generalised-K sum distributions and applications in the performance analysis of equal-gain combining receivers," *IET Commun.*, vol. 5, no. 7, pp. 982–989, May 2011.

[8] P. S. Bithas et al., "On the performance analysis of digital communications over generalized-K fading channels," *IEEE Commun. Lett.*, vol. 10, no. 5, pp. 353–355, May 2006.

[9] R. Narasimhan, "Throughput-delay performance of half-duplex hybrid-ARQ relay channels," in *Proc. IEEE Int. Conf. Commun.*, Beijing, China, May 2008, pp. 986–990.

[10] R. Wang et al., "Performance evaluation of HARQ-assisted hybrid satellite-terrestrial relay networks," *IEEE Commun. Lett.*, vol. 24, no. 2, pp. 423–427, Feb. 2020.

[11] G. Caire and D. Tuninetti, "The throughput of hybrid-ARQ protocols for the Gaussian collision channel," *IEEE Trans. Inf. Theory*, vol. 47, no. 5, pp. 1971–1988, Jul. 2001.

[12] Y. Ruan et al., "Performance evaluation for underlay cognitive satellite-terrestrial cooperative networks," *Sci. China Inf. Sci.*, vol. 61, no. 10, pp. 1–11, Oct. 2018.

[13] I. S. Gradshteyn and I. M. Ryzhik, *Table of Integrals, Series, and Products*, 6th ed. New York, NY, USA: Academic, 2000.